iScience

Article

Shared spectral fingerprints of temporal memory precision and representation of the temporal structure of complex narratives

Graphical abstract

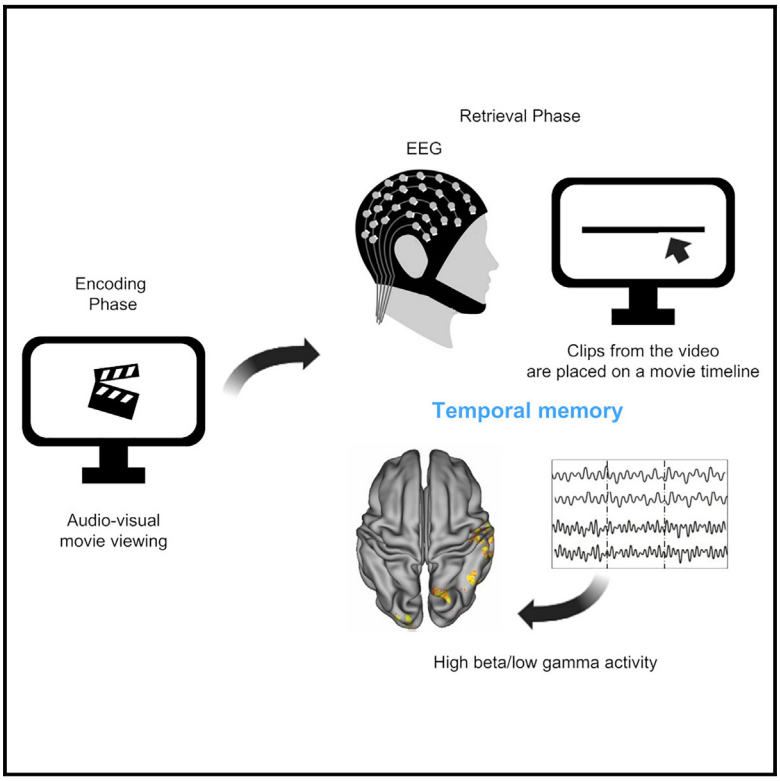

Authors

Matteo Frisoni, Pierpaolo Croce, Annalisa Tosoni, Filippo Zappasodi, Carlo Sestieri

Correspondence

matteo.frisoni3@unibo.it (M.F.), c.sestieri@unich.it (C.S.)

In brief

Neuroscience; Psychology

Highlights

- Temporal memory precision is associated with high beta/low gamma oscillatory activity
- The precision effect is mapped onto a network of right-lateralized regions
- The temporal structure is coded by the same oscillatory activity
- Temporal precision correlates with the temporal structure of the event

Frisoni et al., 2025, iScience *28*, 112132
April 18, 2025
https://doi.org/10.1016/j.isci.2025.112132

CellPress

iScience

CellPress
OPEN ACCESS

Article

Shared spectral fingerprints of temporal memory precision and representation of the temporal structure of complex narratives

Matteo Frisoni,[1,2,3,5,*] Pierpaolo Croce,[1,2] Annalisa Tosoni,[2,4] Filippo Zappasodi,[1,2] and Carlo Sestieri[1,2,*]
[1]Department of Neuroscience, Imaging and Clinical Sciences, Via dei Vestini 11, 66100 Chieti, Italy
[2]ITAB Institute for Advanced Biomedical Technologies, G. d'Annunzio University of Chieti-Pescara, Via dei Vestini 11, 66100 Chieti, Italy
[3]Center for Studies and Research in Cognitive Neuroscience, Department of Psychology "Renzo Canestrari", Cesena Campus, Alma Mater Studiorum University of Bologna, 47521 Cesena, Italy
[4]Department of Psychology, University G. d'Annunzio of Chieti-Pescara, Via dei Vestini 31, 66100 Chieti, Italy
[5]Lead contact
*Correspondence: matteo.frisoni3@unibo.it (M.F.), c.sestieri@unich.it (C.S.)
https://doi.org/10.1016/j.isci.2025.112132

SUMMARY

The ability to date events is fundamental to episodic memory. Separate lines of fMRI research have explored the neurobiological mechanisms underlying temporal precision and the representation of temporal structure in complex events. The present EEG study examined the oscillatory dynamics of both processes in participants performing a timeline positioning task with movie scenes. Multivariate analyses identified a high-beta/low-gamma electrophysiological signature of temporal precision during timeline presentation, involving a right-lateralized network. An independent representation similarity analysis revealed a strong coupling between behavioral and neural distance between pairs of movie parts in the same time-frequency band as the precision effect. Crucially, participants with higher temporal precision showed a stronger correlation between behavioral and neural distance, reinforcing the link between brain signals related to precision and temporal structure representation. These findings support the idea of a systematic temporal organization of experiences, which plays a role in guiding inferential processes.

INTRODUCTION

Temporal context is a defining feature of episodic memories. Animal[1,2] and human[3,4] studies indicate that the entorhinal-hippocampal network plays a crucial role in the processing of temporal memories. Consistent with the idea that hippocampal neuronal ensembles support the temporal organization of episodic memories, recent fMRI studies using multivariate analysis approaches have shown that the human hippocampus differentiates or integrates temporally organized memories, depending on task demands. Specifically, pattern differentiation has been associated with successful retrieval of temporal order and temporal context of encoded information[3,5] whereas pattern similarity has been associated with the learning of temporal associations between events in memory.[6] Following a similar line of research, other studies have shown that hippocampal activity patterns support the incidental and explicit retrieval of both the temporal and spatial context of the encoded event, reflecting the intrinsic spatiotemporal nature of the episodic experience.[7–9] Crucially, this multidimensional coding of memory space is reminiscent of Tolman's original notion of ''cognitive maps'', defined as a systematic organization of experience and knowledge across multiple domains in the service of purposeful behavior.[10]

As research starts to elucidate the neural mechanism underlying memory for time, the field has seen an increased interest in the use of narratives, in contrast to highly controlled but simplified stimuli, as an effective way to ecologically assess the mnemonic representation of complex events on a long timescale.[11–13] For example, Montchal and colleagues[14] asked participants to date snapshots extracted from a previously seen sitcom episode by indicating their time of occurrence on a visual analog scale (VAS) representing the episode timeline. They found that the anterior-lateral entorhinal cortex was more engaged for more precise judgments, supporting its role in processing high-precision temporal memories. However, the results of this study also leave several open questions. Firstly, it is not clear what specific representational mechanism (pattern segregation vs. separation) supports the precision effect and the degree to which the effect reflects more basic or corollary cognitive processes associated with motor preparation, effort, or performance monitoring. Secondly, the human literature has predominantly focused on the hippocampal-entorhinal circuitry, based on evidence for the presence of ''time cells'' in these regions.[1,15] While this circuit possesses the mechanisms required by these temporal computations, other studies have shown that temporal context signals are more spatially distributed,[16,17] and the same might be true for signals related to the representation of the

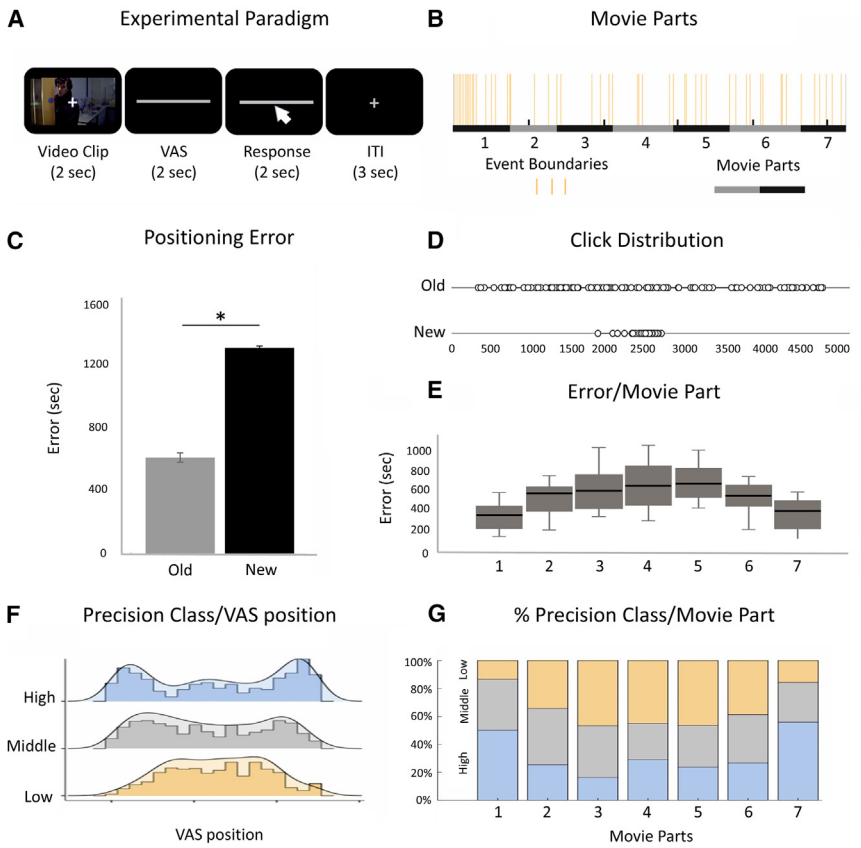

Figure 1. Experimental paradigm and behavioral results

(A) The figure illustrates the experimental paradigm of the time-of-occurrence task. Participants were presented with a series of 2-s video clips, extracted either from the previously encoded episode (old clips) or from unseen, related episodes (new clips). A central white fixation cross was superimposed over the clip. At the offset of the clip, a visual analog scale representing the duration of the whole movie was presented. Participants were asked to wait for the appearance of a cursor and select a point on the horizontal timeline to indicate the exact moment in the movie from which the clip was extracted. They had to left-click a point on the line for clips judged as "old", and right-click for clips judged as "new". An ITI of 3 s with a central fixation cross preceded the next trial.

(B) The position of the event boundaries for each experiment, as determined by an inter-rater analysis in a group of independent observers. The horizontal lines below the graph represent the seven movie parts created for behavioral and EEG data analyses. Note that the edges of the bins correspond to event boundaries.

(C) Mean absolute error for old and new clips across participants. The asterisk indicates the presence of a significant difference. Error bars indicate SEM.

(D) Click distribution for old and new trials. Each circle represents the placement of old (top row) and new (bottom row) clips on the visual analog scale, averaged across participants. The numbers below the line indicate the values of the timeline (in seconds).

(E) Boxplots indicating absolute error as a function of bin/movie part (hits). The horizontal black lines represent the group average. Error bars indicate SEM.

(F) The figure shows the position on the VAS of each trial included in the three precision classes.

(G) The figure illustrates the percentage of trials for the three precision classes in each of the seven movie segments used in the RSA.

temporal structure of complex events. Finally, the functional relationship between brain signals coding for the precision of temporal memories[14] and the representation of the event temporal structure[8,9] is currently unknown, as these phenomena have been investigated in separate lines of research.

In the present study, we exploited the temporal resolution of the EEG technique to identify the brain signals related to temporal memory precision and characterize their temporal, spatial, and spectral properties using a data-driven approach. We found that the oscillatory activity in the high-beta/low-gamma band, measured after the stimulus offset but before manual response, codes for temporal memory precision. A source-level analysis suggested that the effect maps to a network of right-lateralized regions including, but not limited to, the inferior temporal cortex. To examine whether the precision effect relies on a global temporal representation of the narrative, we conducted an independent representation similarity analysis and tested whether the spatial distribution of EEG oscillatory activity carried information about subjective event distance, measured in terms of the positioning of different movie parts on the timeline. This analysis revealed a significant correlation between indices of behavioral and neural distance in the same frequency band and temporal window of the precision effect. Crucially, a significant correlation was observed between the distance effect and temporal memory precision across subjects, further suggesting that the ability to date events relies on the retrieval of a global representation of the narrative.

RESULTS

Twenty right-handed volunteers were asked to watch an episode of the BBC television series Sherlock (Season 1, Episode 1, "A Study In Pink", see in the study by Chen et al.[18]) and, subsequently, to judge the time of occurrence of a series of 2 s video clips extracted from the same or a different episode, by indicating the corresponding point on a VAS representing the episode timeline (Figure 1A). The VAS was presented at the offset of the clip, but subjects had to wait for the appearance of a cursor, i.e., the go signal, to indicate the segment of the timeline. This procedure ensured a time interval of 2 s between the clip offset and the motor response in which only the VAS was present on the screen and the activity related to temporal judgments could be isolated.

Trials were grouped according to signal detection theory,[19] arbitrarily assigning the label "hits" to correctly identified old clips. The relative proportions of trials were the

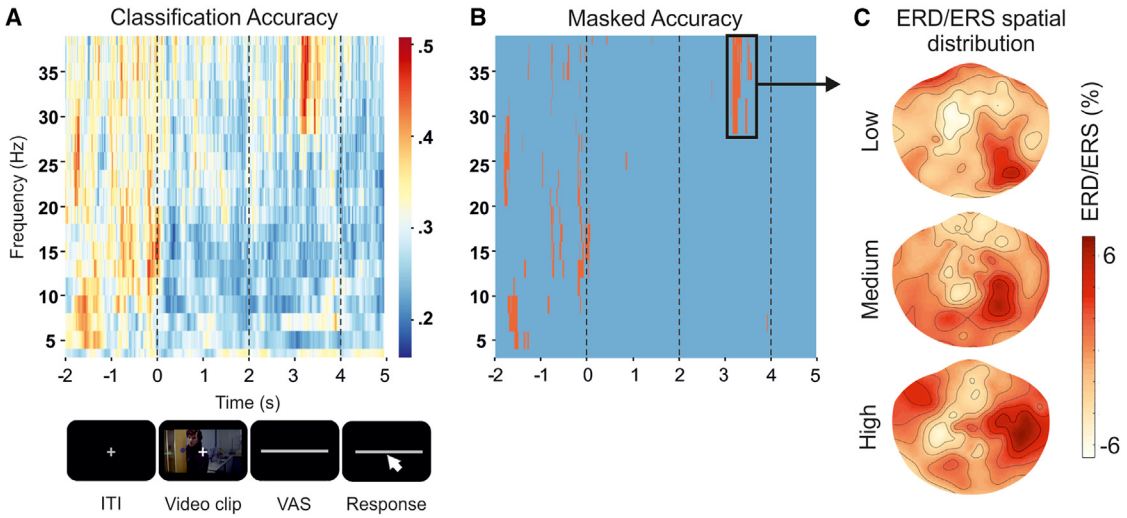

Figure 2. Electrophysiological signature of temporal memory precision

(A) Leave-one-subject-out cross-validated performance of a classifier (linear discriminant analysis) that distinguished between the three levels of temporal memory precision (low, medium, high). The features of the classifier were the ERD/ERS relative to the baseline (i.e., the second preceding the video clip), calculated for each frequency and time point in each EEG channel. The plot illustrates the level of the classifier accuracy as a function of time and frequency. The experimental paradigm is presented below the graph for temporal reference. The boundaries of the different task phases are indicated by dotted lines on the graph.

(B) Time-frequency intervals of classification accuracy that survived a permutation-based analysis against the chance level of 0.33. Orange segments represent time-frequency intervals where a significant classification is observed. The black square indicates the peak of classification accuracy observed in the high-beta/low-gamma band during the VAS presentation interval, after the offset of the video clip, and before the go signal for the manual response.

(C) Average ERD/ERS spatial distribution for low, medium, and high precision trials corresponding to the peak of post-stimulus classification accuracy observed in (B).

following: hits = 0.87 ± 0.10 (mean ± SD); misses = 0.13 ± 0.10; false alarms = 0.05 ± 0.04; correct rejections = 0.95 ± 0.04. We arbitrarily created movie parts for subsequent analyses guided by estimates of event boundaries obtained in an independent group of raters.[13] This subdivision was chosen as the best compromise between the number of movie parts (N = 7) and the number of clips in each part (N = ≈20) for the EEG analyses (Figure 1B, see STAR Methods section for more info about the rationale behind the creation of movie parts).

To ensure that the index of temporal precision reflected a judgment predominantly informed by episodic memory retrieval, and not merely by potential semantic information present in the clips, we compared performance between clips extracted from the encoded (old) vs. unseen (new) movies. Temporal precision was much higher for old (610 s ±133 s; mean absolute error ±SD) compared to new (1302 s ±49 s) clips (Figure 1C) and a paired t-test confirmed the presence of a significant difference [$t(19) = -22.16$, $p = 0.001$], demonstrating the use of a mnemonic representation of the movie to perform the task. Performance for old clips was in line with the result of a previous behavioral study using the same material.[13] Figure 1D shows that, as expected, participants used the entire timeline to report their judgments for old clips, whereas they tended to select central points of the timeline when uncertain or guessing (see in the study by Berliner et al.[20]). A selective repeated measure ANOVA [$F(6,114) = 6.68$, $p < 0.001$] with the movie part as the independent factor revealed that clips extracted from extreme parts (1 and 7) of the encoded movie were positioned more precisely than those from Part 3 to 5 (all $p < 0.05$, Figure 1E). We note that a similar advantage for extreme movie parts has also been observed in studies that minimized the contribution of primacy/recency effects by using a 24-h retention interval[13,21] and thus likely reflects the importance of these parts as landmarks for temporal judgments[22] and narrative structure.[23]

An electrophysiological correlate of temporal memory precision

To identify brain activity related to temporal memory accuracy, we first split correctly identified old trials (hits) of each participant into three categories based on absolute error[14]: high (mean error = 169 ± 114 s), medium- (619 ± 220 s), and low-precision (1761 ± 598 s) trials. The overlap in ranges across classes is due to differences in precision among participants, as the classes were calculated at the individual level. Then, we ran a multivariate pattern analysis (MVPA) of the time-frequency data to identify the distributed pattern of electrical activity that distinguished between these three levels. A linear discriminant analysis (LDA) classifier was applied to measures of power modulation (event related desynchronization/synchronization, ERD/ERS) calculated for each frequency and time point in each EEG channel using a time-frequency generalization analysis. Notably, a leave-one-subject-out approach was employed to identify patterns that could consistently classify temporal memory precision across subjects, thereby focusing on mechanisms shared across subjects. Figure 2A shows the results of the classification analysis, conducted in a temporal interval that started

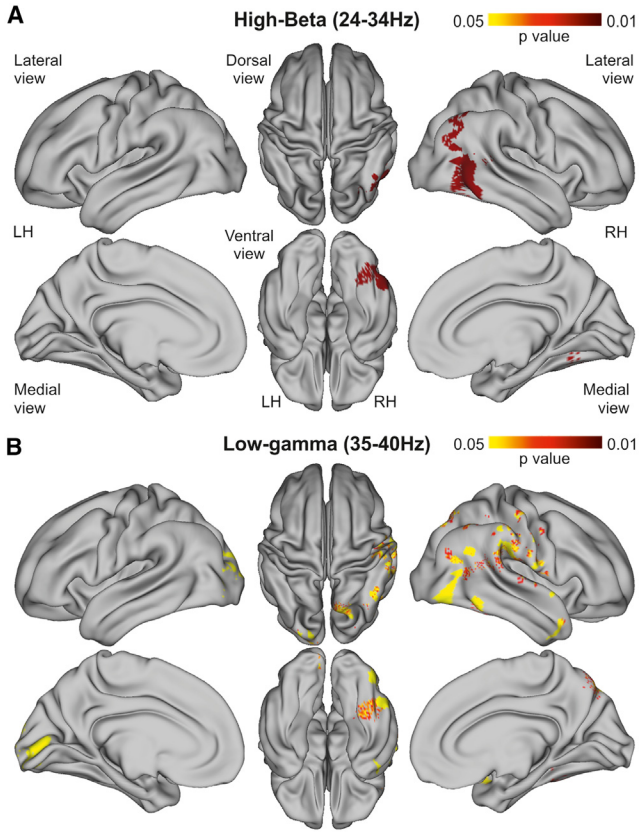

Figure 3. eLORETA source analysis on the peak of precision classification performance

The figure represents a group-level analysis and illustrates the main effect of condition in a within-subject repeated-measure ANOVA with condition (precision levels) as a factor.

(A) Spatial distribution of the precision effect, identified through a whole-brain ANOVA contrasting the ERD/ERS for three conditions (low, medium, and high precision trials) in the high-beta band.

(B) Spatial distribution of the whole-brain ANOVA in the low-gamma band.

2 s before the onset of the clip and ended 3 s after the offset of the clip. Orange spots in the figure indicate peaks of leave-one-subject-out cross validation accuracy. Figure 2B shows the time-frequency intervals of classification accuracy that survive a non-parametric permutation-based test against the chance level of 0.33.

The analysis revealed multiple peaks of classification accuracy in different frequency bands in the time interval preceding the presentation of the clip. Despite effects in the prestimulus baseline are difficult to interpret in the absence of a dedicated experimental paradigm, we propose that this activity might be associated with task preparation, i.e., general attentional/control processes that allow participants to be ready for the upcoming task, whose magnitude can predict subsequent memory performance.[24] However, the most interesting phenomenon was observed in the high-beta/low-gamma frequency band (28–40 Hz) within a time interval that goes from 3 to 3.5 s after the onset of the clip, when only the VAS was present on the screen and before the go-signal for the motor response. The short duration of the temporal window showing the precision effects is notable and was likely caused by the temporal features of the present delay paradigm, which forced participants to wait for the go-signal to report their temporal judgments regardless of when they reached a decision, and by the focus on precision effects shared across subjects, which minimizes interindividual differences. We believe that this high-frequency modulation reflects a shared temporal processing for dating events on a long timescale (minutes to tens of minutes) and the putative electrophysiological counterpart of the precision effect observed in previous fMRI work.[14] The spatial distribution of the electrical activity observed in this interval of the time/frequency domain, corresponding to the three levels of precision, is illustrated in Figure 2C.

Right lateralization of the precision effect

To identify the cortical sources of the precision effect highlighted by the classification approach, we ran an exploratory analysis using eLORETA,[25] focusing on the time-frequency spot illustrated in Figure 2B. For this analysis, we divided the frequency band showing the significant effect into two distinct frequency bands roughly corresponding to classical EEG high-beta (24–34 Hz) and low-gamma (35–40 Hz) bands. Next, we calculated the source distribution of the ERD/ERS in this time/frequency interval for the three levels of precision (high, middle, and low) for the two bands of interest and we conducted a voxelwise ANOVA with precision (high, middle, and low) as the independent factor to localize the precision effect (Figure 3). The source reconstruction algorithm highlighted a significant cluster in the right lateral and inferior temporal cortex for the beta band and a more distributed effect, still largely confined to the right hemisphere but further involving frontal and parietal clusters, for the gamma band. Notably, for both frequency bands, the precision effect involved portions of the right inferior temporal lobe, despite the effect was not centered on medial temporal regions as observed in previous fMRI studies.[14,26–28] While this finding might reflect the lower spatial resolution of the EEG technique to oscillatory modulation in medial compared to lateral structures, the results are consistent with the involvement of a right-lateralized neocortical network in temporal judgments about past events (see also in the study by Montchal et al.[14]).

Spatial processing and motor intentions

As stated in the introduction, multiple cognitive processes might contribute to the manifestation of a precision effect. For example, an important confound for the previous analysis is represented by brain activity related to spatial processing and motor intention. Specifically, the classification of precision levels might potentially reflect the fact that one precision level (i.e., high) is associated with a bias toward processing one side of the VAS and/or planning hand movements to the same side. To exclude the role of spatial and motor processes in the classification of temporal memory precision, we exploited the current experimental design and the temporal resolution of the EEG technique. In particular, we ran a classification analysis on trials divided by the selected position on the VAS (left, center, and right), rather than by precision, to test whether the classification of these signals overlapped with the results of the precision analysis. We

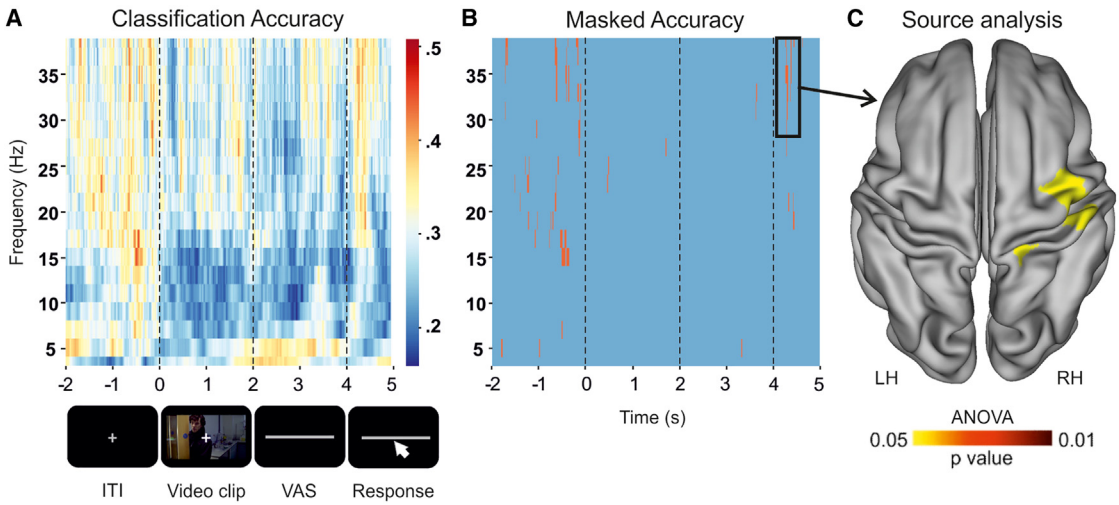

Figure 4. Electrophysiological signature of spatial/motor processing

(A) Leave-one-subject-out cross-validated performance of a classifier (linear discriminant analysis) that distinguishes between trials in which subjects selected different segments of the VAS (left, center, right) to explore the brain activity related to spatial processing and motor intentions. The features of the classifier are the ERD/ERS, relative to the baseline (i.e., the second preceding the video clip), calculated for each frequency and time point in each EEG channel. The plot illustrates the level of the classifier accuracy as a function of time and frequency.

(B) Time-frequency intervals of classification accuracy that survive a permutation-based analysis against the chance level of 0.33. Orange segments represent time-frequency intervals where a significant classification is observed.

(C) Spatial distribution of the effect identified through a whole-brain ANOVA contrasting the ERD/ERS for the three conditions (left, center, right trials) in the high-beta/low gamma band after the go-signal (highlighted in B).

hypothesized that signals related to motor intention should manifest late in the trial, immediately before/after the onset of the go signal.

The results of the analysis revealed the presence of a mild effect of spatial position in the high-beta/low-gamma band, which temporally follows the precision effect (Figure 4). Notably, the peak of the effect, as assessed by the nonparametric permutation test (Figure 4B), was observed after the onset of the go-signal, consistent with the planning of a hand movement toward specific parts of the VAS. A source analysis conducted on the peak of classification performance observed after the go-signal in the low gamma band identified two main clusters located in the somatomotor cortex ipsilateral to the responding hand (Figure 4C), supporting the motor nature of this signal. Overall, these results suggest that the precision effect identified in the main analysis is unlikely to be contaminated by a spatial/motor confound.

Brain representation of the temporal event structure in the time-frequency domain

Another way to infer the computation underlying the precision effect is to examine the brain representation of temporal structure. Despite the participants dated the video clips one at a time, it was still possible to derive a behavioral measure of the perceived distance between different clips by looking at the distribution of clicks on the VAS. This measure could be then compared to the corresponding distance between the patterns of brain electrical activity following the presentation of the clips, to test if the two measures showed a significant relationship in the time-frequency domain. We hypothesized that a positive correlation between behavioral and neural distance, an index of the representation of the temporal structure of the movie, should share some functional properties with the precision effect. Notably, the analysis of temporal precision was performed by sampling trials from the whole VAS, regardless of the movie segment, whereas the analysis of temporal structure was performed by sampling trials from specific movie parts, irrespective of temporal precision. Thus, the two analyses were supposed to be relatively independent from each other (but see the limitations of the study section in the discussion).

The similarity between behavioral and neural distance associated with pairs of movie parts was investigated with a representational similarity analysis (RSA), by averaging all the trials belonging to each of the seven movie parts. A behavioral matrix was created for each participant (Figure 5A), representing the perceived distance between movie parts in terms of the difference in positioning (number of segments) on the VAS. A series of neural matrices for each frequency bin and moment in time were also created for each participant (Figure 5B), representing the distance between movie parts in terms of differences in the spatial distribution of the ERD/ERS across all channels. We then tested when, and in which frequency, a significant correlation between measures of behavioral and neural distance was observed. Figure 5C shows the Pearson correlation coefficient between the vectorized matrices of behavioral and neural distance calculated for each frequency and time point. Crucially, the analysis revealed a strong coupling at approximately the same time and frequency band compared to the precision effect (compared with Figure 2A). This effect survived a permutation-based analysis against null correlation (Figure 5D). Figure 5E

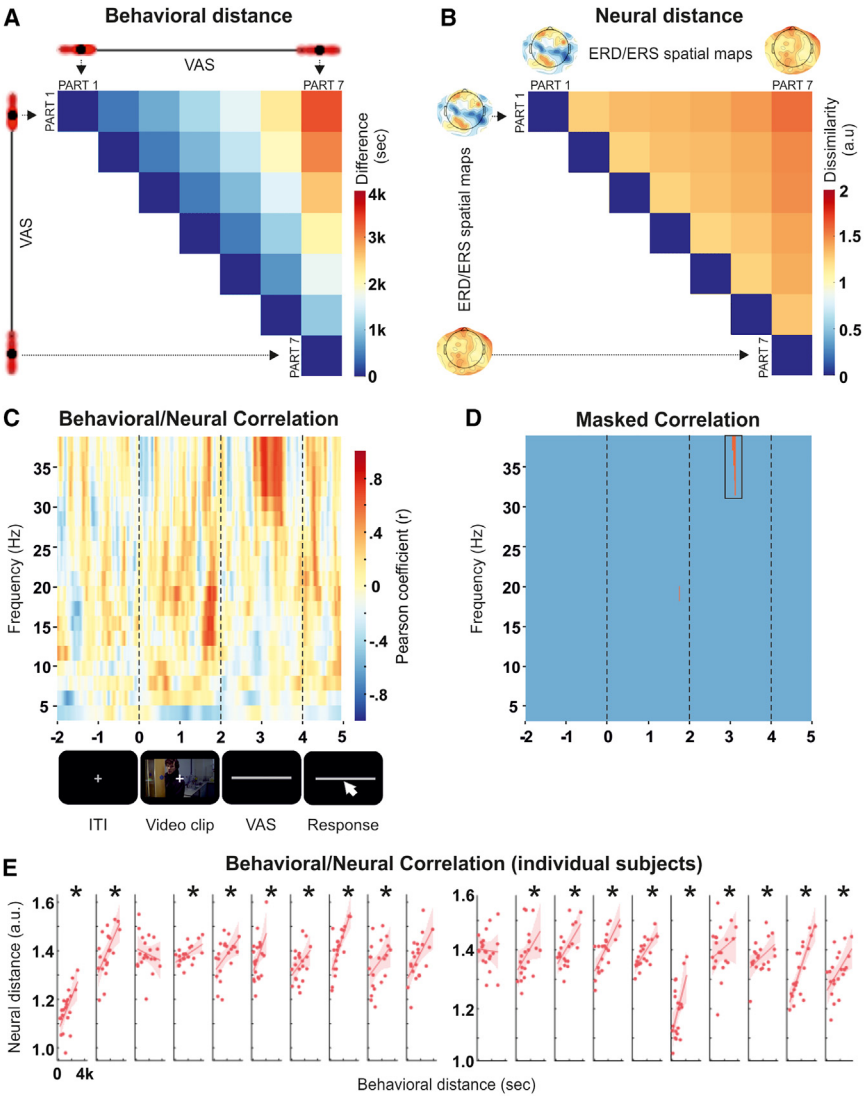

Figure 5. Correlation between behavioral and neural distance

(A) Behavioral distance between movie parts. The matrix represents the difference between the average positioning on the VAS for each pair of movie parts across subjects.

(B) Neural distance between movie parts. The dissimilarity matrix represents the distance between the average ERD/ERS distributions for each pair of movie bins (1—spatial correlation) across subjects.

(C) Time-frequency intervals of correlation across matrices of behavioral and neural distance.

(D) Time-frequency intervals of significant correlation across matrices of behavioral and neural distance that survive a permutation-based analysis against null correlation. Red segments represent time-frequency intervals where a significant correlation is observed.

(E) Scatterplots of the correlation between behavioral and neural distance in each subject, calculated in the point of the time/frequency representation highlighted in (D). The asterisks indicate statistically significant correlations.

illustrates the scatterplot of the correlation between behavioral and neural distance in this interval of the time-frequency domain for each participant. Indeed, a significant correlation was observed in 18/20 participants.

Taken together, these findings indicate that movie parts judged to be closer in time elicited more similar distributions of low-gamma activity than distant movie parts. We believe that the higher similarity between movie parts that were closer in time unlikely reflects the contribution of low-level perceptual features, as the beginning/ends of the movie parts coincided with event boundaries obtained from independent raters, to avoid the splitting of the same scene into two consecutive parts and the eventual inflation of the similarity between adjacent segments. Instead, we propose that this behavioral-neural relationship is an index of the representation of the temporal structure of the movie, which remarkably overlaps in time and frequency with the precision effect. In this respect, the results of the RSA analysis provide an independent confirmation that the precision effect truly reflects a temporal computation and helps to distinguish the function of the post-stimulus precision effect from that of the pre-stimulus counterpart.

Relationship between temporal precision and the neural representation of event structure

Since the temporal precision and temporal structure effects shared the same frequency band and time point, we explored the nature of the relationship between the two findings. We conducted a Spearman skipped correlation to ascertain the robustness of the association and observed a significant correlation between the two variables, after the exclusion of one outlier [$r_{skipped}$ = −0.54, CI (−0.86, −0.05); Figure 6].

DISCUSSION

Neural mapping of temporal memory precision and event temporal structure

A hallmark of episodic memory is the representations of events in specific spatiotemporal contexts,[29] and the hippocampal formation is considered a key structure in coding locations in space and moments in time (reviewed in[30,31]). Recently, distinct research lines have started to investigate the role of the medial temporal lobe (MTL) in temporal memory performance and the representation of the temporal structure of complex events. Focusing on precision, Montchal and colleagues[14] have shown that the anterior-lateral entorhinal cortex was more engaged for more precise judgments, supporting its role in processing high-precision temporal memories during explicit retrieval.

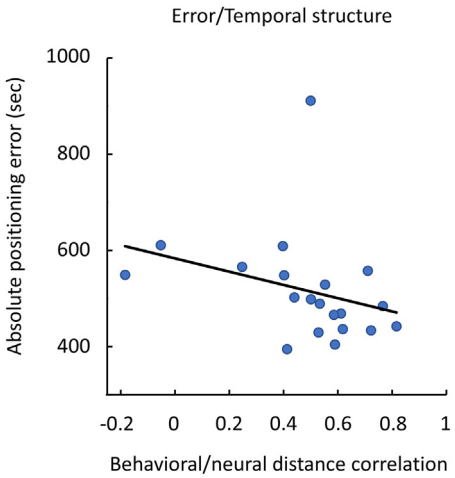

Figure 6. Correlation between behavioral/neural distance and the absolute positioning error

Scatterplot showing the relationship between behavioral/neural temporal distance and the absolute positioning error.

Concerning temporal representations, multivariate analysis approaches have shown that the remembered spatiotemporal proximity is encoded in hippocampal-entorhinal activity pattern,[8,9] suggesting an abstract and flexible representation of the external world.[32] Of note, whereas activation studies on temporal memory precision (i.e., temporal positioning of memory items on the VAS representing the episode duration) are based on activity contrasts between different levels of temporal memory performance, imaging studies based on multivariate analysis approaches have focused on the automatic reactivation of a representational dimension (i.e., structure) and content of temporal memory. More in general, while these two lines of evidence converge on the crucial role of the MTL in temporal memory, it remains unclear if, and how, the representation aspect of episodic memory supports task performance in difficult temporal memory tasks.

Using ecological narrative material and multivariate analyses of EEG data, here we combined the analysis of evoked activity associated with different levels of temporal memory precision with the analysis of the organizational structure of temporal memory. Firstly, we showed that the temporal memory precision is associated with activity in the high-beta/low-gamma band (28–40 Hz) that occurs approximately 1000–1500 ms after the offset of the visual stimulus, is shared across subjects, and is independent of spatial processing and motor intention. Secondly, using a representation similarity analysis, we identified a consistent relationship across subjects between indices of behavioral and neural distance. We think that the overlap, in terms of both timing and frequency, between the precision and the distance effects, and the presence of a significant relationship between behavioral indices of temporal precision and the distance effect, is remarkable, given that the two analyses are both data-driven. The present results allow us to trace an important link between independent lines of research focusing on temporal memory performance and event structure, supporting the notion that the precision of temporal memory is based on the reconstruction of the event structure.

Of note, the selective overlap between the distance effect and the precision effect observed post-stimulus further helps to disentangle these modulations from other effects, such as prestimulus modulations, that potentially reflect the active preparation for the upcoming memory task.[24,33,34] At a more theoretical level, although the present study did not directly test a role for a temporal schema in memory for time, previous behavioral[13,21] and imaging[35] research has suggested that participants apply prior knowledge of temporal patterns (schema) when performing temporal positioning tasks. Here, we found that subjects with higher temporal precision were those who also showed a stronger correlation between behavioral and neural distance, i.e., a better representation of temporal structure. On this basis, we speculate that the beta/gamma signal represents a kind of "gateway" to a reference template that helps the positioning task.

Spatial distribution of the high-beta/low-gamma activity

The fMRI literature on temporal memory precision[14] and event structure[8,9] has mainly focused on BOLD activity within ROIs located in the MTL, based on the electrophysiological properties exhibited by the hippocampal-entorhinal circuitry.[1,36] However, a close association has been reported between hippocampal gamma and neocortical oscillations during both memory encoding and retrieval.[37,38] The source localization analysis conducted in the present EEG study indicates that the temporal precision effect was observed in a network of regions that include the inferior temporal cortex, close but not overlapping with the classical entorhinal-hippocampal circuit. We acknowledge that the role of the MTL might have been underestimated by the present source analysis approach, due to the intrinsic spatial limitations of the EEG technique.[39] However, the involvement of a wide network of neocortical regions, and the presence of an evident rightward asymmetry, are consistent with previous findings obtained in several fMRI studies addressing temporal memory with complex audiovisual material[40,41] or mental time travel.[42] In particular, the study by Lohnas and colleagues[43] has been the first to demonstrate a neural correlate of temporal context in scalp EEG. They presented words in sequence and computed an "event vector"[44] on 42 channels and 46 frequencies for each presented stimulus. The features that autocorrelated between different event vectors were those that defined a common context (i.e., a slowly changing temporal context[44,45]). In addition, they showed that the temporal context associated with a word was reinstated at retrieval. Our findings are consistent with this evidence and extend the results to complex audiovisual material. Moreover, the similarity between temporal contexts in Lohnas' study was measured in relative terms, as no "typical" temporal context frequency was identified. In our case, the overall structure of the material (i.e., the whole movie) was considered, and thus the focus was on the "global" temporal structure rather than the "local" temporal context. Taken together, these results suggest that oscillatory components of temporal context can be found at the cortical level at multiple scales ("local" vs. "global").

Furthermore, our work provides information on the spatial localization of this effect and extends the findings of previous

research on time perception to a larger temporal scale. Indeed, it has been shown that temporal information is widely distributed across frontoparietal regions and that the right parietal cortex is associated with accurate temporal estimation.[46] While the involvement of the MTL in the temporal memory of complex events has been demonstrated by the aforementioned fMRI studies, our study also suggests the importance of a distributed cortical network that has only been traced for tasks with subsecond stimuli.[46] A limitation of the present study is that it does not allow us to explore the interaction between hippocampal-entorhinal circuits and neocortical areas, or the specific function of each region involved, but it suggests that multiple neural systems support the timing function.[47,48] Furthermore, our results highlight the rightward asymmetry suggested by previous studies using simpler materials such as word lists,[49] and different tasks (before/after judgments[49]; distance judgments between two clips of a story[50]; self-projection in time/mental time travel[51]). Taken together, the available evidence indicates that temporal judgments are more likely to be associated with rightward activation, even at larger time scales such as that used in the present study.

Mapping of temporal sequences

In addition to encoding and retrieving episodes within global event representations that support performance in temporal positioning and temporal distance tasks, the hippocampal formation is also thought to play a role in remembering the order of events in specific experiences,[2,32] allowing the spatiotemporal evolution of episodes over longer timescales to be predicted from individual "snapshots", i.e., mental time travel.[52,53] Consistently, human fMRI studies have provided compelling evidence that hippocampal activity patterns encode information associated with specific sequences of events.[3,5,28,54] These findings have supported the idea that similarity or differentiation between hippocampal activity is largely determined by the task at hand,[7] i.e., whether behavioral performance is based on similarity[6] or differentiation[3,5] between temporally arranged memory items.

Concerning the oscillatory mechanisms underlying the coding of event sequences, the theoretical account of Buzsáki and Moser[55] proposes that both spatial and temporal sequences are coded by cell firing that occurs at troughs of theta-rhythm cycle, a phenomenon called theta phase precession.[56] Specifically, sequence encoding is thought to be supported by interactions between high- and low-frequency oscillations. Theta-phase modulation of gamma power has been shown to correlate with memory performance in both rats and humans.[57–60] In this regard, our work may complement previous evidence from a MEG study by Heusser and colleagues,[61] who studied sequence encoding (memory for order, i.e., encoding of items in distinct sequence positions) and found that this process is supported by progressive shifts in gamma power along the phase of theta modulation. These findings suggest that the brain encodes the order of a sequence of items by integrating gamma-coded item representations with the theta-phase-coded item ordinal position. Furthermore, the interaction between theta and gamma activity was centered in the left hippocampus and extended posteriorly to a region of the parahippocampal and fusiform gyrus, suggesting a role for the hippocampus and surrounding MTL cortical regions in sequence encoding.[3,28] In contrast to the evidence obtained at encoding, we observed a rightward beta-gamma mechanism for memory retrieval. Future studies are needed to investigate the nature of the differential contribution of distinct frequency bands across different phases of the memory task.

Moreover, it is worth noting that the requirements of the temporal task may explain the involvement of different temporal memory mechanisms. Indeed, although sequence encoding appears to be a fundamental mechanism of episodic memory supported by the hippocampal-entorhinal region,[62] we emphasize that the kind of temporal information processing in the present paradigm is less related to temporal order memory (relative times of occurrence, e.g., recency judgments[22]) and more related to location or distance processes,[22] that occur when participants are asked to reconstruct the position of an event within a global representation (e.g., timeline positioning task[13,21]). We therefore speculate that the beta/gamma activity observed in the present work might reflect a different/complementary phenomenon compared to the theta/gamma interaction for temporal order memory.

A unifying framework linking temporal memory precision and representation of event structure

According to several frameworks (see[30,63]), place and grid population codes in the MTL provide a representational format to map variable dimensions of cognitive spaces.[62,64] Specifically, a reconciliation between the memory and spatial views of hippocampal functions has been advanced, revisiting the original notion of cognitive maps as a multi-dimensional map of event space that encodes positions along dimensions of experience beyond the Euclidean space for navigation.[10] Within this proposal, information about specific episodes is abstracted and represented at a higher level of granularity compared to the individual episodes.[32] As a result, finer-scale representations of temporally closer episodic fragments (e.g., "snapshot") become more similar and integrated into mnemonic networks, giving rise to the automatic reactivation of associated representations.

Consistent with the idea that the cognitive map is in the service of optimal behavior, the memory space can directly support task performance. Our findings are consistent with this notion of a map-like temporal organization of the narrative, in which the degree of integration vs. segregation of distributed activity patterns is associated with both the remembered proximity of different story segments and the global precision in the temporal positioning task. Based on the pivotal observations of Buzsaki and Moser,[55] we speculate that the timeline positioning emphasizes the structuring of temporal knowledge in a map-like organization and the encoding of positional information in a "static" reference frame (i.e., a global representation in which positions can be flexibly represented at different spatial scale and granularity level). Unfortunately, the spatial limitations of the EEG technique did not allow us to directly infer conclusions about the involvement of the hippocampus but extend the theoretical frameworks of an event map of memory space at the level of distributed brain networks. Together, our results

fit well with the notion of a "memory space" or "cognitive map", in which events and episodes are organized within relational networks, e.g., the narrative's temporal structure, to satisfy specific behavioral purposes, such as the temporal positioning of video clips along the movie timeline.

Limitations of the study

One limitation of the present study concerns the temporal resolution of the analyses. Despite temporal precision being assessed with great accuracy at the behavioral level, due to intrinsic limitations of the EEG technique, trials were grouped into only three classes for the precision analysis. Similarly, the RSA analysis was performed by averaging trials within seven movie parts to maximize signal to noise ratio (SNR). However, future studies employing more trials should be aimed at increasing the temporal resolution of the present results.

A second limitation concerns the independence between the precision and the temporal structure analyses. While the two analyses were based on a different grouping of trials, we cannot completely exclude the issue represented by their potential interdependence, as temporal precision was not uniform across the VAS (Figure 1E), and the proportion of trials from the three precisions classes reflected this asymmetry. However, we note that the inverse u-shaped relationship between precision and movie segments makes it unlikely that the similarity between segments reflects temporal precision, e.g., extreme segments should be judged as closer due to their higher precision.

Conclusion

The present study suggests a role for high-beta/low-gamma frequency in coding for both temporal memory precision and the representation of event structure. These effects occurred simultaneously after stimulus presentation but before the manual response and were observed in a distributed cortical network beyond the MTL. Taken together, our results help to link different phenomena reported in the literature on temporal memory and shed new light on how complex events in our life become "infused with time".

RESOURCE AVAILABILITY

Lead contact

Further information and requests for resources should be directed to and will be fulfilled by the lead contact, Matteo Frisoni (matteo.frisoni3@unibo.it).

Materials availability

This study did not generate new unique reagents.

Data and code availability

- Original data have been deposited on Mendeley at https://data.mendeley.com/datasets/kckpk2yrtg/1 and are publicly available as of the date of publication. DOIs are listed in the key resources table.
- All original code has been deposited on Mendeley and is publicly available at https://data.mendeley.com/datasets/rd686vmr46/1 as of the date of publication.
- Any additional information required to reanalyze the data reported in this paper is available from the lead contact upon request.

ACKNOWLEDGMENTS

We thank Danilo De Iure for help with data collection. This work was supported by a grant awarded to M. Frisoni from the Bial Foundation [grant number 384/20] and was conducted under the framework of the Departments of Excellence 2018–2022 initiative of the Italian Ministry of Education, University and Research for the Department of Neuroscience, Imaging and Clinical Sciences (DNISC) of the University of Chieti-Pescara. This research received external funding from "PRIN: PROGETTI DI RICERCA DI RILEVANTE INTERESSE NAZIONALE" (Research project title: "EEG connectivity as an innovative biomarker to improve QUAlity of LIfe and The burden of disease in people with drug resistant epilepsY (EQUALITY)"; Prot. P20225HWLZ; CUP: D53D23019080001), Bando 2022 PNRR, D.D. n. 1409/2022, funded by European Union - NextGenerationEU (Missione 4, Componente 2, Investimento 1.1.); P.I.: F. Zappasodi.

AUTHOR CONTRIBUTIONS

M.F. and C.S conceived the study. M.F. and C.S. developed and implemented the experimental setup. M.F. performed the experiment. P.C. provided technical support during the experiment. M.F., P.C., C.S., and F.Z. performed data analysis. M.F., C.S., P.C., and A.T. wrote the manuscript. F.Z. provided technical consultation for the revision of the manuscript. All authors drafted and approved the final version of the manuscript.

DECLARATION OF INTERESTS

The authors declare no conflict of interest.

STAR★METHODS

Detailed methods are provided in the online version of this paper and include the following:

- KEY RESOURCES TABLE
- EXPERIMENTAL MODEL AND STUDY PARTICIPANT DETAILS
- METHOD DETAILS
  - Materials
  - Procedure
  - Identification of movie parts
- QUANTIFICATION AND STATISTICAL ANALYSIS
  - Behavioral analyses
  - EEG recordings and data processing
  - Preprocessing and time-frequency computation
  - Classification analyses
  - ERD/ERS source reconstruction
  - Representational similarity analysis
  - Correlation between memory precision and the neural representation of temporal structure

Received: June 19, 2024
Revised: December 14, 2024
Accepted: February 26, 2025
Published: March 1, 2025

REFERENCES

1. MacDonald, C.J., Lepage, K.Q., Eden, U.T., and Eichenbaum, H. (2011). Hippocampal "time cells" bridge the gap in memory for discontiguous events. Neuron *71*, 737–749. https://doi.org/10.1016/j.neuron.2011.07.012.
2. Eichenbaum, H. (2014). Time cells in the hippocampus: a new dimension for mapping memories. Nat. Rev. Neurosci. *15*, 732–744. https://doi.org/10.1038/nrn3827.

3. Davachi, L., and DuBrow, S. (2015). How the hippocampus preserves order: the role of prediction and context. Trends Cognit. Sci. *19*, 92–99. https://doi.org/10.1016/j.tics.2014.12.004.

4. Bellmund, J.L.S. (2020). Piecing Together Cognitive Maps One Dimension at a Time. Neuron *107*, 996–999. https://doi.org/10.1016/j.neuron.2020.08.014.

5. Ezzyat, Y., and Davachi, L. (2014). Similarity breeds proximity: pattern similarity within and across contexts is related to later mnemonic judgments of temporal proximity. Neuron *81*, 1179–1189. https://doi.org/10.1016/j.neuron.2014.01.042.

6. Schapiro, A.C., Kustner, L.V., and Turk-Browne, N.B. (2012). Shaping of object representations in the human medial temporal lobe based on temporal regularities. Curr. Biol. *22*, 1622–1627. https://doi.org/10.1016/j.cub.2012.06.056.

7. Copara, M.S., Hassan, A.S., Kyle, C.T., Libby, L.A., Ranganath, C., and Ekstrom, A.D. (2014). Complementary roles of human hippocampal subregions during retrieval of spatiotemporal context. J. Neurosci. *34*, 6834–6842. https://doi.org/10.1523/JNEUROSCI.5341-13.2014.

8. Deuker, L., Bellmund, J.L., Navarro Schroder, T., and Doeller, C.F. (2016). An event map of memory space in the hippocampus. Elife *5*, 16534. https://doi.org/10.7554/eLife.16534.

9. Bellmund, J.L., Deuker, L., and Doeller, C.F. (2019). Mapping sequence structure in the human lateral entorhinal cortex. Elife *8*, e45333. https://doi.org/10.7554/eLife.45333.

10. Tolman, E.C. (1948). Cognitive maps in rats and men. Psychol. Rev. *55*, 189–208.

11. Lee, H., Bellana, B., and Chen, J. (2020). What can narratives tell us about the neural bases of human memory? Curr. Opin. Behav. Sci. *32*, 111–119.

12. Nastase, S.A., Goldstein, A., and Hasson, U. (2020). Keep it real: rethinking the primacy of experimental control in cognitive neuroscience. Neuroimage *222*, 117254. https://doi.org/10.1016/j.neuroimage.2020.117254.

13. Frisoni, M., Di Ghionno, M., Guidotti, R., Tosoni, A., and Sestieri, C. (2021). Reconstructive nature of temporal memory for movie scenes. Cognition *208*, 104557. https://doi.org/10.1016/j.cognition.2020.104557.

14. Montchal, M.E., Reagh, Z.M., and Yassa, M.A. (2019). Precise temporal memories are supported by the lateral entorhinal cortex in humans. Nat. Neurosci. *22*, 284–288. https://doi.org/10.1038/s41593-018-0303-1.

15. Pastalkova, E., Itskov, V., Amarasingham, A., and Buzsáki, G. (2008). Internally generated cell assembly sequences in the rat hippocampus. Science *321*, 1322–1327. https://doi.org/10.1126/science.1159775.

16. El-Kalliny, M.M., Wittig, J.H., Jr., Sheehan, T.C., Sreekumar, V., Inati, S.K., and Zaghloul, K.A. (2019). Changing temporal context in human temporal lobe promotes memory of distinct episodes. Nat. Commun. *10*, 203. https://doi.org/10.1038/s41467-018-08189-4.

17. Folkerts, S., Rutishauser, U., and Howard, M.W. (2018). Human Episodic Memory Retrieval Is Accompanied by a Neural Contiguity Effect. J. Neurosci. *38*, 4200–4211. https://doi.org/10.1523/JNEUROSCI.2312-17.2018.

18. Chen, J., Leong, Y.C., Honey, C.J., Yong, C.H., Norman, K.A., and Hasson, U. (2017). Shared memories reveal shared structure in neural activity across individuals. Nat. Neurosci. *20*, 115–125. https://doi.org/10.1038/nn.4450.

19. Green, D.M., and Swets, J.A. (1966). Signal Detection Theory and Psychophysics (New York: Wiley).

20. Berliner, J.E., Durlach, N.I., and Braida, L.D. (1977). Intensity perception. VII. Further data on roving-level discrimination and the resolution and bias edge effects. J. Acoust. Soc. Am. *61*, 1577–1585. https://doi.org/10.1121/1.381471.

21. Frisoni, M., Di Ghionno, M., Guidotti, R., Tosoni, A., and Sestieri, C. (2023). Effects of a narrative template on memory for the time of movie scenes: Automatic reshaping is independent of consolidation. Psychol. Res. *87*, 598–612.

22. Friedman, W.J. (1993). Memory for the Time of Past Events. Psychol. Bull. *113*, 44–66.

23. Cutting, J., and Iricinschi, C. (2015). Re-presentations of space in Hollywood movies: An event-indexing analysis. Cogn. Sci. *39*, 434–456.

24. Park, H., and Rugg, M.D. (2010). Prestimulus hippocampal activity predicts later recollection. Hippocampus *20*, 24–28. https://doi.org/10.1002/hipo.20663.

25. Pascual-Marqui, R.D. (2007). Discrete, 3D distributed, linear imaging methods of electric neuronal activity. Part 1: Exact, zero error localization. Preprint at arXiv. https://doi.org/10.48550/arXiv.0710.3341.

26. Jenkins, L.J., and Ranganath, C. (2010). Prefrontal and medial temporal lobe activity at encoding predicts temporal context memory. J. Neurosci. *30*, 15558–15565. https://doi.org/10.1523/JNEUROSCI.1337-10.2010.

27. Tubridy, S., and Davachi, L. (2011). Medial temporal lobe contributions to episodic sequence encoding. Cerebr. Cortex *21*, 272–280. https://doi.org/10.1093/cercor/bhq092.

28. Hsieh, L.T., and Ranganath, C. (2015). Cortical and subcortical contributions to sequence retrieval: Schematic coding of temporal context in the neocortical recollection network. Neuroimage *121*, 78–90. https://doi.org/10.1016/j.neuroimage.2015.07.040.

29. Tulving, E. (1983). In Elements of Episodic Memory (Oxford University Press).

30. Schiller, D., Eichenbaum, H., Buffalo, E.A., Davachi, L., Foster, D.J., Leutgeb, S., and Ranganath, C. (2015). Memory and Space: Towards an Understanding of the Cognitive Map. J. Neurosci. *35*, 13904–13911. https://doi.org/10.1523/JNEUROSCI.2618-15.2015.

31. Milivojevic, B., and Doeller, C.F. (2013). Mnemonic networks in the hippocampal formation: from spatial maps to temporal and conceptual codes. J. Exp. Psychol. Gen. *142*, 1231–1241. https://doi.org/10.1037/a0033746.

32. Eichenbaum, H., Dudchenko, P., Wood, E., Shapiro, M., and Tanila, H. (1999). The hippocampus, memory, and place cells: is it spatial memory or a memory space? Neuron *23*, 209–226. https://doi.org/10.1016/s0896-6273(00)80773-4.

33. Addante, R.J., de Chastelaine, M., and Rugg, M.D. (2015). Pre-stimulus neural activity predicts successful encoding of inter-item associations. Neuroimage *105*, 21–31. https://doi.org/10.1016/j.neuroimage.2014.10.046.

34. de Chastelaine, M., and Rugg, M.D. (2015). The effects of study task on prestimulus subsequent memory effects in the hippocampus. Hippocampus *25*, 1217–1223. https://doi.org/10.1002/hipo.22489.

35. Bellmund, J.L.S., Deuker, L., Montijn, N.D., and Doeller, C.F. (2022). Mnemonic construction and representation of temporal structure in the hippocampal formation. Nat. Commun. *13*, 3395. https://doi.org/10.1038/s41467-022-30984-3.

36. McNaughton, B.L., Battaglia, F.P., Jensen, O., Moser, E.I., and Moser, M.B. (2006). Path integration and the neural basis of the 'cognitive map. Nat. Rev. Neurosci. *7*, 663–678. https://doi.org/10.1038/nrn1932.

37. Griffiths, B.J., and Jensen, O. (2023). Gamma oscillations and episodic memory. Trends Neurosci. *46*, 832–846. https://doi.org/10.1016/j.tins.2023.07.003.

38. Hanslmayr, S., Staresina, B.P., and Bowman, H. (2016). Oscillations and Episodic Memory: Addressing the Synchronization/Desynchronization Conundrum. Trends Neurosci. *39*, 16–25. https://doi.org/10.1016/j.tins.2015.11.004.

39. Michel, C.M., and Brunet, D. (2019). EEG Source Imaging: A Practical Review of the Analysis Steps. Front. Neurol. *10*, 325. https://doi.org/10.3389/fneur.2019.00325.

40. Lositsky, O., Chen, J., Toker, D., Honey, C.J., Shvartsman, M., Poppenk, J.L., Hasson, U., and Norman, K.A. (2016). Neural pattern change during encoding of a narrative predicts retrospective duration estimates. Elife *5*, e16070. https://doi.org/10.7554/eLife.16070.

41. Kwok, S.C., and Macaluso, E. (2015). Immediate memory for "when, where and what": Short-delay retrieval using dynamic naturalistic material. Hum. Brain Mapp. *36*, 2495–2513. https://doi.org/10.1002/hbm.22787.

42. Gauthier, B., and van Wassenhove, V. (2016). Time Is Not Space: Core Computations and Domain-Specific Networks for Mental Travels. J. Neurosci. *36*, 11891–11903. https://doi.org/10.1523/JNEUROSCI.1400-16.2016.

43. Lohnas, L.J., Healey, M.K., and Davachi, L. (2023). Neural temporal context reinstatement of event structure during memory recall. J. Exp. Psychol. Gen. *152*, 1840–1872. https://doi.org/10.1037/xge0001354.

44. Manning, J.R., Polyn, S.M., Baltuch, G.H., Litt, B., and Kahana, M.J. (2011). Oscillatory patterns in temporal lobe reveal context reinstatement during memory search. Proc. Natl. Acad. Sci. USA *108*, 12893–12897. https://doi.org/10.1073/pnas.1015174108.

45. Howard, M.W., and Kahana, M.J. (2002). A distributed representation of temporal context. J. Math. Psychol. *46*, 269–299.

46. Hayashi, M.J., van der Zwaag, W., Bueti, D., and Kanai, R. (2018). Representations of time in human frontoparietal cortex. Commun. Biol. *1*, 233.

47. Wiener, M., Turkeltaub, P., and Coslett, H.B. (2010). The image of time: a voxel-wise meta-analysis. Neuroimage *49*, 1728–1740. https://doi.org/10.1016/j.neuroimage.2009.09.064.

48. Wiener, M., Matell, M.S., and Coslett, H.B. (2011). Multiple mechanisms for temporal processing. Front. Integr. Neurosci. *5*, 31.

49. Cabeza, R., Mangels, J., Nyberg, L., Habib, R., Houle, S., McIntosh, A.R., and Tulving, E. (1997). Brain Regions Differentially Involved in Remembering What and When: a PET Study. Neuron *19*, 863–870.

50. Lositsky, O., Chen, J., Toker, D., Honey, C.J., Shvartsman, M., Poppenk, J.L., Hasson, U., and Norman, K.A. (2016). Neural pattern change during encoding of a narrative predicts retrospective duration estimates. Elife *5*, e16070.

51. Gauthier, B., and van Wassenhove, V. (2016). Cognitive mapping in mental time travel and mental space navigation. Cognition *154*, 55–68.

52. Tulving, E. (1972). In Organization of memory (Academic Press).

53. Tulving, E. (2002). Episodic memory: from mind to brain. Annu. Rev. Psychol. *53*, 1–25. https://doi.org/10.1146/annurev.psych.53.100901.135114.

54. Kalm, K., Davis, M.H., and Norris, D. (2013). Individual sequence representations in the medial temporal lobe. J. Cognit. Neurosci. *25*, 1111–1121. https://doi.org/10.1162/jocn_a_00378.

55. Buzsaki, G., and Moser, E.I. (2013). Memory, navigation and theta rhythm in the hippocampal-entorhinal system. Nat. Neurosci. *16*, 130–138. https://doi.org/10.1038/nn.3304.

56. O'Keefe, J., and Recce, M.L. (1993). Phase relationship between hippocampal place units and the EEG theta rhythm. Hippocampus *3*, 317–330. https://doi.org/10.1002/hipo.450030307.

57. Tort, A.B.L., Komorowski, R.W., Manns, J.R., Kopell, N.J., and Eichenbaum, H. (2009). Theta-gamma coupling increases during the learning of item-context associations. Proc. Natl. Acad. Sci. USA *106*, 20942–20947. https://doi.org/10.1073/pnas.0911331106.

58. Axmacher, N., Henseler, M.M., Jensen, O., Weinreich, I., Elger, C.E., and Fell, J. (2010). Cross-frequency coupling supports multi-item working memory in the human hippocampus. Proc. Natl. Acad. Sci. USA *107*, 3228–3233. https://doi.org/10.1073/pnas.0911531107.

59. Canolty, R.T., Edwards, E., Dalal, S.S., Soltani, M., Nagarajan, S.S., Kirsch, H.E., Berger, M.S., Barbaro, N.M., and Knight, R.T. (2006). High gamma power is phase-locked to theta oscillations in human neocortex. Science *313*, 1626–1628. https://doi.org/10.1126/science.1128115.

60. Griesmayr, B., Gruber, W.R., Klimesch, W., and Sauseng, P. (2010). Human frontal midline theta and its synchronization to gamma during a verbal delayed match to sample task. Neurobiol. Learn. Mem. *93*, 208–215. https://doi.org/10.1016/j.nlm.2009.09.013.

61. Heusser, A.C., Poeppel, D., Ezzyat, Y., and Davachi, L. (2016). Episodic sequence memory is supported by a theta-gamma phase code. Nat. Neurosci. *19*, 1374–1380. https://doi.org/10.1038/nn.4374.

62. Bellmund, J.L.S., Gardenfors, P., Moser, E.I., and Doeller, C.F. (2018). Navigating cognition: Spatial codes for human thinking. Science *362*, eaat6766. https://doi.org/10.1126/science.aat6766.

63. Milivojevic, B., and Doeller, C.F. (2013). Mnemonic networks in the hippocampal formation: from spatial maps to temporal and conceptual codes. J. Exp. Psychol. Gen. *142*, 1231–1241. https://doi.org/10.1037/a0033746.

64. Igarashi, K.M., Lu, L., Colgin, L.L., Moser, M.B., and Moser, E.I. (2014). Coordination of entorhinal-hippocampal ensemble activity during associative learning. Nature *510*, 143–147. https://doi.org/10.1038/nature13162.

65. Baldassano, C., Chen, J., Zadbood, A., Pillow, J.W., Hasson, U., and Norman, K.A. (2017). Discovering Event Structure in Continuous Narrative Perception and Memory. Neuron *95*, 709–721. https://doi.org/10.1016/j.neuron.2017.06.041.

66. Newtson, D., and Engquist, G. (1976). The perceptual organization of ongoing behavior. J. Exp. Soc. Psychol. *12*, 436–450.

67. Radvansky, G.A., and Zacks, J.M. (2017). Event Boundaries in Memory and Cognition. Curr. Opin. Behav. Sci. *17*, 133–140. https://doi.org/10.1016/j.cobeha.2017.08.006.

68. Ester, M., Kriegel, H.-P., Sander, J., and Xu, X. (1996). A density-based algorithm for discovering clusters in large spatial databases with noise. In KDD ' 96: Proceedings of the second international conference on knowledge discovery and data mining, pp. 226–231.

69. Barbati, G., Porcaro, C., Zappasodi, F., Rossini, P.M., and Tecchio, F. (2004). Optimization of an independent component analysis approach for artifact identification and removal in magnetoencephalographic signals. Clin. Neurophysiol. *115*, 1220–1232. https://doi.org/10.1016/j.clinph.2003.12.015.

70. Croce, P., Zappasodi, F., Marzetti, L., Merla, A., Pizzella, V., and Chiarelli, A.M. (2019). Deep Convolutional Neural Networks for Feature-Less Automatic Classification of Independent Components in Multi-Channel Electrophysiological Brain Recordings. IEEE Trans. Biomed. Eng. *66*, 2372–2380. https://doi.org/10.1109/TBME.2018.2889512.

71. Munoz, A., Ertle, R., and Unser, M. (2002). Continuous wavelet transform with arbitrary scales and O(N) complexity. Signal Process. *82*, 749–757.

72. Pfurtscheller, G., and Lopes da Silva, F.H. (1999). Event-related EEG/MEG synchronization and desynchronization: basic principles. Clin. Neurophysiol. *110*, 1842–1857. https://doi.org/10.1016/s1388-2457(99)00141-8.

73. Arieli, A., Sterkin, A., Grinvald, A., and Aertsen, A. (1996). Dynamics of ongoing activity: Explanation of the large variability in evoked cortical responses. Science *273*, 1868–1871.

74. Buzsáki, G., Anastassiou, C.A., and Koch, C. (2012). The origin of extracellular fields and currents — EEG, ECoG, LFP, and spikes. Nat. Rev. Neurosci. *13*, 407–420.

75. Blankertz, B., Lemm, S., Treder, M., Haufe, S., and Müller, K.-R. (2011). Single-trial analysis and classification of ERP components—a tutorial. Neuroimage *56*, 814–825.

76. Cichy, R.M., Pantazis, D., and Oliva, A. (2014). Resolving human object recognition in space and time. Nat. Neurosci. *17*, 455–462.

77. Treder, M.S. (2020). MVPA-Light: A Classification and Regression Toolbox for Multi-Dimensional Data. Front. Neurosci. *14*, 289. https://doi.org/10.3389/fnins.2020.00289.

78. Tominaga, Y. (1999). Comparative study of class data analysis with PCA-LDA, SIMCA, PLS, ANNs, and k-NN. Chemometr. Intell. Lab. Syst. *49*, 105–115.

79. Fahrenfort, J.J., van Driel, J., van Gaal, S., and Olivers, C.N.L. (2018). From ERPs to MVPA Using the Amsterdam Decoding and Modeling Toolbox (ADAM). Front. Neurosci. *12*, 368. https://doi.org/10.3389/fnins.2018.00368.

80. Zhang, Y., and Yang, Y. (2015). Cross-validation for selecting a model selection procedure. J. Econom. *187*, 95–112.

81. Oostenveld, R., and Oostendorp, T.F. (2002). Validating the boundary element method for forward and inverse EEG computations in the presence of a hole in the skull. Hum. Brain Mapp. *17*, 179–192. https://doi.org/10.1002/hbm.10061.

82. Kriegeskorte, N., Mur, M., and Bandettini, P. (2008). Representational similarity analysis - connecting the branches of systems neuroscience. Front. Syst. Neurosci. *2*, 4. https://doi.org/10.3389/neuro.06.004.2008.

83. Kaneshiro, B., Perreau Guimaraes, M., Kim, H.S., Norcia, A.M., and Suppes, P. (2015). A Representational Similarity Analysis of the Dynamics of Object Processing Using Single-Trial EEG Classification. PLoS One *10*, e0135697. https://doi.org/10.1371/journal.pone.0135697.

84. Pernet, C.R., Wilcox, R., and Rousselet, G.A. (2012). Robust correlation analyses: False positive and power validation using a new Open Source Matlab Toolbox. Front. Psychol. *3*, 606. https://doi.org/10.3389/fpsyg.2012.00606.

STAR★METHODS

KEY RESOURCES TABLE

REAGENT or RESOURCE	SOURCE	IDENTIFIER
Deposited data		
Dataset	This paper	https://data.mendeley.com/datasets/kckpk2yrtg/1
Software and algorithms		
Statistica v10	Statsoft	http://www.statsoft.com/Products/STATISTICA/Product-Index
MATLAB	Mathworks	www.mathworks.com/products/MATLAB.html
EEGLAB	OpenSource	sccn.ucsd.edu/eeglab/
FieldTrip	OpenSource	www.fieldtriptoolbox.org/
Scripts	Mendeley.com	https://data.mendeley.com/datasets/rd686vmr46/1

EXPERIMENTAL MODEL AND STUDY PARTICIPANT DETAILS

Twenty right-handed volunteers (11 females; aged 20–30 years; mean age: 22.7 years), unfamiliar with the movie show, participated in the study. Participants were naive as to the purpose of the experiment, reported normal or corrected-to-normal vision, and gave informed consent before the experiment according to the guidelines of the Human Studies Committee of the G. d'Annunzio University of Chieti. The study consisted of three sessions (Figure 1) and lasted for a total of approximately 3 h in total: pre-movie passive viewing of movie clips (∼30 min), movie encoding (∼90 min), and timeline positioning task (∼45 min). The three sessions were separated by a 5-min break. EEG recording was performed during the first and third sessions. For the present manuscript, only data from the third session (memory retrieval) were analyzed.

METHOD DETAILS

Materials

The stimuli consisted of video clips of 2-s duration. Old stimuli (N = 140) were extracted from an episode of the TV show "Sherlock" (BBC One, 2010, season #1, episode #1: "A Study In Pink"; duration: 87:30 min) dubbed in Italian. Stimuli were sampled uniformly every 36.75 s (time-locked to the center of the clip). NEW stimuli (N = 140) were taken from other unseen episodes of the same series as multiples of 36.75 s and were somewhat uniformly distributed: we divided each episode into quarters of about 22 min and used 5/6 clips randomly taken from each quarter. A first subset of NEW stimuli (N = 70) was used for the pre-movie session (Season #1, Episode #3: N = 23; Season #2, Episode #1: N = 24; Season #3, Episode #3: N = 23), while a second subset (N = 70) was used for the retrieval phase (Season #1, Episode #2: N = 23; Season #2, Episode #3: N = 23; Season #3, Episode #1: N = 24). A central white fixation cross was superimposed on each clip. After the clip presentation, a central horizontal gray line (size: 0.9 ° × 19.8 ° visual angle), representing the duration of the movie, appeared at the center of the screen. The line consisted of 1000 consecutive segments, each corresponding to 5.25 s of the movie. The experiment was performed in a darkened testing room. Stimuli were presented on a 17′ LCD computer monitor (1024 × 768 pixels, 60 Hz refresh rate) at a distance of ∼60 cm. Subjects listened to the audio track at a comfortable level (∼60 dB).

Procedure

During the pre-movie session, participants were asked to passively view a series of randomly presented video clips. Each clip was followed by an intertrial interval (ITI) of 3 s. Participants were instructed to attend to the clips but were not informed about the nature of the following tasks. The EEG data for this session was not analyzed for this manuscript. In the movie session (encoding), the episode of the BBC television series Sherlock (Season 1, Episode 1). They were instructed to pay attention to the episode but were not told the nature of the following task. In the post-movie session (retrieval), participants were presented with a series of video clips (N = 210; old clips: N = 140; new clips: N = 70) and performed a combined item recognition/timeline positioning task. The order of the video clips was randomized across subjects. Each trial began with the presentation of the video clip at the center of the screen (Figure 1A). A central white fixation cross was superimposed over the clip. The clip was followed by the presentation of the VAS for 2 s. Participants were asked to wait for the onset of an arrow pointer to select a point on the timeline with a mouse click and indicate the exact moment in the movie from which the clip was taken. They were asked to click with the left mouse button (index finger) for clips judged as "old" and with the right mouse button (middle finger) for clips judged as "new" (recognition judgment). Therefore, participants were encouraged to indicate the time of occurrence also of clips they had not seen. The pointer remained on the screen for 2 s and was followed by an intertrial interval (ITI) of 3 s. No feedback was provided. The instructions made clear that the line represented the duration of the

movie that was presented in the encoding session, in a left (beginning) to right (end) direction. An experimenter made sure that the subjects understood the instructions during the practice session.

Identification of movie parts

To quantify variations of performance as a function of the clip position, we split the movie into seven movie parts (bins) that lasted on average 12.5 min (750 ± 48 s; mean ± SD, Figure 1B). This division was based on the results of a pilot experiment, described by,[13] in which an independent group of 20 participants overtly segmented the video with the following indications[65]: "Write down the times at which you feel like a new scene is starting; these are points in the movie when there is a major change in topic, location, time, etc. Also, give each scene a short title". This procedure is thought to reveal the spontaneous viewers' segmentation of ongoing narratives into sub-parts, i.e., events ,[66] and a good agreement in the positioning of event boundaries across subjects has been previously demonstrated.[67]

Event boundaries were extracted with a data-driven method by using the DBSCAN clustering algorithm.[68] After the removal of outlier annotations, the algorithm automatically identified the best number of clusters based on two parameters: the number of observations and the temporal window. Specifically, clusters were identified by counting at least ten observations following (within 2.5 s) and preceding (within 2.5 s) a randomly chosen annotation (total temporal window = 5 s). Boundaries were obtained by averaging all the observations within each identified cluster. This procedure identified 52 event boundaries that were most characteristic of the group of observers. Next, we arbitrarily divided the movie into seven bins, aiming for the best compromise between number of bins, consistency of bin duration and presence of a sufficient number of clips in each bins (20 on average; Bin 1: $N = 19$; Bin 2: $N = 18$; Bin 3: $N = 19$; Bin 4: $N = 21$; Bin 5: $N = 21$; Bin 6: $N = 21$; Bin 7: $N = 21$).

Importantly, event boundaries were too frequent and unevenly distributed across the movie, making it impractical to base the subdivision of movie parts solely on them. At the same time, the intentional coincidence between the beginning/end of an arbitrary segment and the presence of an event boundary prevented a scene (i.e., an event) from being split into two segments, thus avoiding potential inflation of the similarity index between adjacent segments due to perceptual similarity. To test whether judgments about the time of occurrence were more precise as a function of proximity to event boundaries,[13] we ran a trial-by-trial Spearman Rank Order Correlation Test between the group-level absolute error for each clip and the corresponding clip distance from the nearest boundary. The correlation was not significant (rs = 0.07, $p = 0.38$).

QUANTIFICATION AND STATISTICAL ANALYSIS

Behavioral analyses

Statistical analyses were conducted using Statistica Software v10 (http://www.statsoft.com/Products/STATISTICA/Product-Index) and MATLAB (www.mathworks.com/products/matlab) toolbox. Analyses were conducted on 4090 out of 4200 trials due to a malfunction of the EEG trigger during the recordings of two participants (40 trials for one, 70 trials for the other). The precision of temporal memory was calculated as the temporal distance in absolute value, quantified in seconds, between the line segment selected by the subject and the correct segment for each trial, relative to the center of each video clip. We first conducted a paired-sample t-test to determine if the amount of absolute error was significantly different between old and new stimuli across participants. Then, we used the bin as an independent variable in a 1-way repeated-measures analysis of variance (ANOVA) on precision for correctly recognized old clips to assess whether performance varied across movie parts. Tukey HSD Post Hoc tests were used to test differences across bins. Correlations between the vectorized matrices of behavioral and neural distance calculated for each frequency and time point were performed using Pearson's correlation.

EEG recordings and data processing

EEG activity was recorded using a 128-channel system (Electrical Geodesic) during the pre-movie and retrieval sessions. Electrode impedance was kept below 50 kΩ. EEG data were sampled at 250 (1–80 Hz filtering) and collected for offline processing.

Preprocessing and time-frequency computation

Data were pre-processed using EEGLAB toolbox. The data underwent visual inspection to exclude saturated EEG signal epochs from further analysis. A semi-automatic method, using Independent Component Analysis,[69,70] was employed to detect and eliminate ocular, cardiac, and muscular artifacts. Subsequently, the signals were re-referenced to the common average. Data were filtered between 1 and 45 Hz, were downsampled at 125 Hz, and were segmented into epochs starting from 2000 ms before the clip onset and lasting 5000 ms after the clip offset. Time-frequency representation (TFR) was computed for each EEG channel using a continuous Complex Morlet transformation[71] in the 3–40 Hz range, at 1 Hz of frequency resolution. TFR was obtained as the squared magnitude of the complex wavelet-transformed data. Power modulations (Event-Related Desynchronization/Synchronization, ERD/ERS) were quantified as percentage change compared to the baseline period, i.e., the 2000 ms of the pre-stimulus period:

$$ERD\,/\,ERS \;=\; 100(P_t - P_b)\,/\,P_b$$

where P_t was the TFR value at any given time-frequency value, and P_b the mean power in the baseline period.

Classification analyses

Data were processed using custom MATLAB codes, EEGLAB and Fieldtrip toolboxes. A multivariate pattern analysis (MVPA) was used to classify the distributed pattern of ERD/ERS as a function of temporal precision, measured at the behavioral level. MVPA aims to 'decode' brain activity by predicting a model from the data. This method differs from classical approaches as it considers multiple variables (channels, time, and frequencies) simultaneously, rather than treating them as independent entities (as done in classical Event-Related Potential or Time-Frequencies analysis.[72] The objective of the decoding analysis was to test whether it was possible to predict temporal memory precision across three levels of precision based on the spatial-temporal-spectral structure of the EEG data. The underlying assumption was that if time-frequency EEG activity can successfully predict whether a trial corresponds to a specific level of precision, it is possible to conclude that the spatiotemporal pattern of ERS/ERD at a given frequency encodes information about temporal memory. It should be noted that the decision to consider three precision groups has a methodological rationale. Indeed, compared to fMRI, single-trial estimates are rarely used in EEG due to the lower SNR.[73,74] Therefore, even if temporal memory was measured with high precision, we averaged a sufficient number of trials per class to obtain meaningful results. Furthermore, classification analyses are usually applied to two classes, in part because increasing the number of classes creates problems for the interpretation of the results.[75,76] Despite these limitations, the use of a leave-one-subject-out classification allowed us to test three levels of precision across subjects. Correctly recognized old EEG trials were split into three levels of precision, based on absolute error: low (<33° percentile), medium (between the 33° and the 67° percentile), and high (>67 percentile) trials. The ERD/ERS calculated for each channel, time point, and frequency for the three levels of precision were used as features for the classifier. MVPA was conducted using the MVPA-Light MATLAB toolbox.[77] Specifically, a three-class Linear Discriminant Analysis (LDA)[78] classifier was trained for each time-frequency point of the EEG data, employing a time-frequency generalization analysis.[79] Considering NC EEG channels, NT time instant, and NF frequency bins, the total number of LDA classifier input features was NCxNTxNF. The output of the time-frequency generalization analysis yielded a value of accuracy for each time and frequency. The LDA was trained in a Leave-One-Out (Subject) Cross Validation (LOO-CV) framework.[80] Trials from each subject and level of precision were averaged and the LDA model was trained on all data from all subjects except one in an iterative manner. The out-of-sample performance (i.e., generalization) was assessed based on the remaining subjects and averaged across iterations. To determine if the accuracy achieved by the classifier was statistically different from the chance accuracy level (33% in the present case), a non-parametric permutation test was carried out. Specifically, the training and test procedure was repeated 10,000 times, shuffling the labels of the trials (low, medium, and high precision). An empirical density probability distribution was generated for each time point and for each frequency and accuracy values higher than the 99th percentile of the distributions were considered as significantly different from chance with a $p < 0.01$.

As a control analysis on the effect of spatial processing and motor intention, the same classification analysis was repeated on trials divided as a function of the subjective positioning on the VAS (left, center, right), rather than by level of precision.

ERD/ERS source reconstruction

To determine the underlying cortical sources of the TFR maps, we applied eLORETA[25] to the TFR representation in the time-frequency window corresponding to the peak of the poststimulus precision effect. The volume conductor model was derived from a boundary element method (BEM)[81] of a template brain (http://www.bic.mni.mcgill.ca/ServicesAtlases/Colin27, Accessed on 10 February 2021), and the source space was modeled by a Cartesian 3D grid bounded by the template anatomy with 5113 voxels. Visualization of cerebral sources was performed using the connectome workbench (https://www.humanconnectome.org/software/connectome-workbench). To identify the distribution of the precision effect in the source reconstructed space, we performed a three-way repeated measure ANOVA with precision level as the within-subjects factor.

Representational similarity analysis

Data were processed using custom MATLAB code, EEGLAB and Fieldtrip toolbox. The neural representation of event temporal structure was investigated using a Representational Similarity Analysis (RSA)[82] applied to EEG data.[83] RSA is a data analysis technique used to examine the similarity of neural representations across different experimental conditions or stimuli. The analysis is especially useful when investigating high-dimensional and complex neural data, as it allows us to focus on global patterns of brain activity rather than focusing on specific brain regions. In this study, the RSA analysis aimed to find a significant relationship between the representation of different movie parts observed at the behavioral and neural level, through a measure of distance. For each subject, we calculated two matrices, one reflecting the neural distance (1 - the similarity in the spatiotemporal electrical activity at a specific time interval and frequency) and one reflecting the behavioral distance (difference between average positioning on the VAS) between pairs of movie parts. Importantly, the measure of neural distance reflected the global dissimilarity (DISS) between the EEG spatial configuration corresponding to the specific pairs of movie parts, quantified as the configuration variations between two electric fields, regardless of their strengths. This parameter was calculated as the square root of the average of the squared differences between the potentials recorded at each electrode (relative to the average reference). DISS can vary between 0 (topographical configurations are opposite) and 2 (identical topographical configurations).

To evaluate the presence of a significant relationship between measures of neural and behavioral distance, we correlated, for each subject, the RSA superior matrix for each time and for each frequency specified by the time-frequency analysis, producing a final time-frequency correlation map. To determine if the correlation values were significant, a non-parametric permutation test was

carried out. Specifically, the same correlation analysis was repeated 10,000 times, shuffling the order of movie parts. An empirical density probability distribution was generated for each time point and each frequency and correlation value higher than the 99th percentile of the distributions were considered as significantly different from zero with a $p < 0.01$.

Correlation between memory precision and the neural representation of temporal structure

To test for the presence of a relationship between the behavioral measure of temporal memory precision and the neural representation of temporal structure, we performed a Spearman skipped correlation between measures of absolute positioning error and coupling between behavioral and neural distance across subjects. Skipped correlation were performed using the Robust Correlation toolbox,[84] conducting null hypothesis statistical significance testing using the non-parametric bootstrap percentile test (2000 samples, 95% confidence interval, corresponding to an alpha level of 0.05). This method removes outliers and guarantees a more robust estimate of the association between the variables under consideration. The method identified one outlier.